Supplementary Information (SI) for ChemComm.

Supporting information

Activation of biochar by CO_2 produced from same pyrolysis process and captured *in-situ* by CaO

Mengjiao Fan[a], Yuewen Shao[a], Chao Li[a], Yuchen Jiang[a], Yunyu Guo[a], Shu Zhang[b], Kai Sun[c], Yi Wang[d], Xun Hu[a,*]

[a]School of Material Science and Engineering, University of Jinan, Jinan, 250022, P. R. China.

[b]Joint International Research Laboratory of Biomass Energy and Materials, College of Materials Science and Engineering, Nanjing Forestry University, Nanjing, 210037, PR China.

[c]School of Chemistry and Chemical Engineering, University of Jinan, 250022, P.R. China.

[d]State Key Laboratory of Coal Combustion, Huazhong University of Science and Technology, P.R. China

*Corresponding author. E-mail: Xun.Hu@outlook.com (X. Hu).

1. Materials and methods

1.1 Materials

The willow branch (WB) used herein was obtained from the campus of University of Jinan (China). The WB were firstly dried to constant weight and subsequently ground into fine particle of 0.5–1 mm. CaO was purchased from China National Pharmaceutical Group Corporation Chemical Reagent Co., Ltd. All the chemical agents are analytical grade.

1.2 Experimental procedures

The pyrolysis or activation experiment was conducted in a fixed-bed reactor. Before experiment, N_2 with a flow rate of 60 mL/min was used to purge the reactor to remove residual air, which was also used as a protective gas in pyrolysis or activation. For activation of the biochar from pyrolysis of WB, CaO and WB were mixed at a mass ratio of 1 : 1 and ground thoroughly (> 10 min). Then 4 g of the mixture was placed at outlet of the quartz reactor. When the reactor was heated to 600°C, the mixture was pushed into center of the quartz reactor and held for 30 min. The volatiles generated in this process were trapped by three gas-liquid separators that immersing in ice water. The bio-oil was condensed in the first two gas-liquid separators and the last one that containing ethanol was used for further capturing the uncondensed volatiles. The gaseous product was collected in a gas bag for the further analysis.

After cooling down the reactor, the biochar was collected and weighted for calculation of its yield. After this, the solid was further heated to 900°C with a ramping rate of 10 ºC/min and held for 1 h in a N_2 flow. The biochar, bio-oil and gas formed in this process were also collected with the procedure described above. Especially, the biochar produced from subsequent pyrolysis at 900°C was further washed with 2 M HCl solution and denoted as activated carbon (AC), aiming to remove the Ca species remained inside biochar. For control experiment, the pyrolysis of WB was also performed in the absence of CaO at both 600 and 900°C. The experiments were repeated for three times for verifying accuracy of the result. The yield of biochar, bio-oil, and gas were calculated by using the following formulas:

For the pyrolysis at 600°C: the feedstock was biomass in the presence/absence of CaO. For the subsequent pyrolysis at 900°C: the feedstock was biochar obtained from the pyrolysis of 600°C.

$$Y_{biochar} = \frac{m_{bc}}{m_{feedstock}} \times 100 \quad (1)$$

m_{bc}: mass of biochar after pyrolysis; $m_{feedstock}$: mass of feedstock in the presence/absence of CaO.

$$Y_{AC} = \frac{m_{AC}}{m_{biomass}} \times 100 \quad (2)$$

m_{AC}: mass of biochar after pickling; $m_{biomass}$: mass of only biomass

$$Y_{bio\text{ - }oil} = \frac{m_{bo}}{m_{feedstock}} \times 100 \quad (3)$$

m_{bo}: mass of bio-oil after reaction

$$Y_{gas} = 100\% - (Y_{biochar} + Y_{bio\text{ - }oil}) \quad (4)$$

1.3 Characterizations

Gases were analyzed with GC-7920 instrument (Zhongjiao Jinyuan, China) to quantitatively measure abundance of each gaseous component. The light and heavy components of bio-oil were characterized by gas chromatography-mass spectrometry (GC-MS) instrumentation (Shimadzu GC-MS-QP, Japan) and UV-fluorescence spectroscopy (Shimadzu, RF-6000, Japan). Brunauer–Emmet–Teller (Biaode SSA-6000), X-ray diffraction (Rigaku Ultima IV, Japan), Elemental analyzer (European A3000-Single, Italy), Thermogravimetric instrument (HCT-1, Hengjiu, China), Fourier transform infrared spectroscopy (Nicolet iS50), Contact angle goniometer (Powereach, JC2000D1), Scanning electron microscopy (SEM, Japan) were used to analyze systematically the physicochemical properties of biochar/AC. Especially, the evolution of functionalities on the surface of nascent biochar was investigated with in-situ

DRIFTS (Nicolet iS50, America) to reflect the participation mechanism of CaO in the whole process.

1.4 Tetracycline adsorption

The performance of both the biochar formed at 600°C and AC formed at 900°C for adsorption of tetracycline was measured. Different mass of biochar/AC (10 to 50 mg) with an increment of 10 mg was added to tetracycline solution of 50 mg/L, which was shaken at 200 r/min for 1 h for sufficient adsorption. The solution was then centrifuged and the supernatant was separated for further analysis. The concentration of tetracycline solution before and after adsorption was determined by UV-visible spectrophotometer (Shimadzu, UV-2600i). The removal percentage (R%) of phenol was calculated by the following formula:

$$R\% = \frac{C_0 - C_e}{C_0} \times 100\% \qquad (5)$$

in which C_0 and C_e are the initial and final concentrations tetracycline (mg L^{-1}), respectively.

2.Characterization of biochars/ACs

2.1 Elemental analysis

Table S2 shows the results for the elemental analysis of the biochars and ACs obtained from the subsequent pyrolysis at 900ºC. The addition of CaO enhanced condensation in the initial step of pyrolysis of 600ºC, and the released CO_2 from $CaCO_3$ decomposition further etched the carbonaceous component at 900ºC. These two processes jointly affected evolution of elements in ACs, especially H and O. Specifically, the presence of CaO led to enrichment of oxygen in the WB-CaO-AC-900, resulting in the decreased C/O ratios. Additionally, the CaO also led to retainment of H in the pyrolysis of WB, forming the AC with lower C/H ratios.

2.2 TG analysis

Decomposition of WB as well as the biochar at 600 or 900ºC were analyzed with TG characterization (Figure S2). The pyrolysis of WB could be mainly divided into the first stage at 250–350ºC for decomposition of cellulose/hemicellulose with a high weight loss rate and a second stage above 350ºC for decomposition of lignin with rigid structure with a relative slow weight loss rate. The addition of CaO resulted in the delay of weight loss in the first stage, which was related to the reactions of CaO with CO_2 and organics as well as the condensation reactions catalyzed by CaO. For thermal treatment of biochar, the weight loss peak at 718ºC was attributed to the further cracking of carbonaceous component at high temperature. In comparison, the large weight loss of the biochar from the co-pyrolysis of CaO and WB at 780ºC was ascribed to decomposition of the formed $CaCO_3$. Besides, AC showed lower thermal stability than the counterpart biochar. This might because the presence of CaO decreased the aromatic degree of the derived ACs, as indicated by the lower ratios of C/H and C/O (Table S2). Furthermore, the remained calcium species might continue to catalyze cracking of organics, resulting in the lower thermal stability.

2.3 Contact angle analysis

The hydrophilic/hydrophobic nature of WB, biochars and ACs was reflected by contact angle analysis with water droplet (Figure S3). The introduction of CaO improved the adsorption of water droplets by WB, due to its strong hygroscopicity. Intense dehydration and carbonization occurred in the pyrolysis at 600ºC, resulting in a much higher degree of hydrophobicity on the surface of biochar. Nevertheless, the formed $CaCO_3$ made the biochar more hydrophilic. Even though the subsequent pyrolysis of 900ºC further enhanced the aromatization degree of the biochar, the derived ACs were still more hydrophilic, attributing to the formation of more porous structures from the cracking.

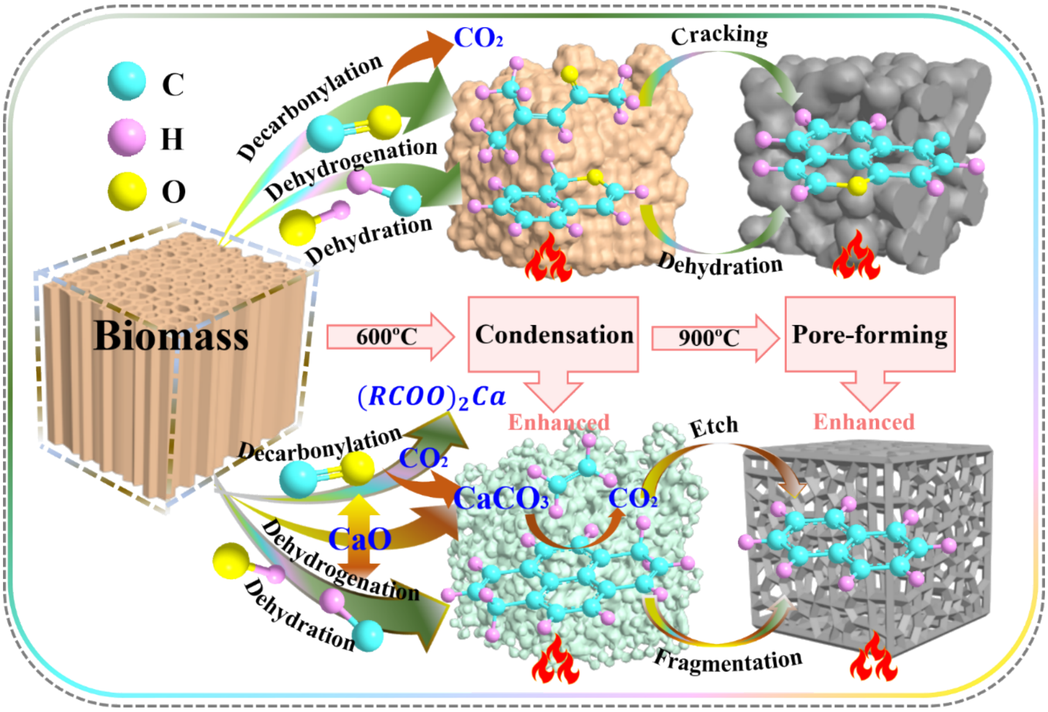

Scheme S1 Proposed mechanism for functionality evolution and pore creation in the pyrolysis of biomass in the presence of CaO.

Table S1 The relative abundance of light organics in the bio-oil produced from pyrolysis of willow branch with/without CaO at 600°C

	Compound	Relative abundance to methyl tetradecanoate(%)	
		WB	**WB+CaO**
Acids	Acetic acid	5.7	0.21
Esters	Acetic acid, hydroxy-, ethyl ester	1.6	0
	2-Oxepanone	0.86	0
	Butyrolactone	0	0.2
	Diethoxymethyl acetate	0.34	0
Ketones	2-Propanone, 1-hydroxy-	2.4	0.82
	2-Butanone, 1-(acetyloxy)-	1.1	0
	2-Propanone, 1-(acetyloxy)-	0.62	0
	1,2-Cyclopentanedione	1.2	0
	2-Cyclopenten-1-one, 3-methyl-	0.22	0.43
	2-Cyclopenten-1-one, 2-hydroxy-3-methyl-	1.14	0.43
	2-Cyclopenten-1-one, 3-ethyl-2-hydroxy-	0.57	0.14
	4-Hydroxy-2-methylacetophenone	1.2	0
	2-Cyclopenten-1-one, 2,3-dimethyl-	0	0.28
	2-Cyclopenten-1-one, 3,4,4-trimethyl-	0	0.12
	2-Cyclopenten-1-one, 3,4,4-trimethyl-	0	0.12
	2-Propanone, 1-(4-hydroxy-3-methoxyphenyl)-	0.46	0
	3',5'-Dimethoxyacetophenone	0.86	0.28
Aldehydes	Propanal	0.71	0
Ethers	Di-n-propyl ether	0.77	0
	Benzene, 1,2,3-trimethoxy-5-	0.34	0

	methyl-		
Furans	3-Furanmethanol	1.2	0
	2,4-Dimethylfuran	0.85	0
	Furfural	2.0	0
Alcohols	Cyclopropyl carbinol	0.87	0
Sugars	1,4:3,6-Dianhydro-.alpha.-d-glucopyranose	0.38	0.09
	.beta.-D-Glucopyranose, 1,6-anhydro-	2.58	0.62
Phenols	Phenol	2.92	1.07
	Phenol, 2-methyl-	0.97	0.49
	p-Cresol	1.17	0.54
	Phenol, 2-methoxy-	0.77	0.29
	Phenol, 2,4-dimethyl-	0.31	0.29
	Phenol, 3-ethyl-	0.00	0.19
	Creosol	0.00	0.35
	Phenol, 2-ethoxy-	2.31	0.00
	1,4-Benzenediol, 2-methoxy-	2.24	0.00
	Phenol, 4-ethyl-2-methoxy-	0.52	0.13
	1,2-Benzenediol, 4-methyl-	1.42	0.37
	2-Methoxy-4-vinylphenol	0.00	0.48
	Phenol, 2,6-dimethoxy-	1.59	0.47
	Eugenol	1.92	0.28
	1,3-Benzenediol, 4-ethyl-	1.01	0.26
	Phenol, 2-methyl-6-(2-propenyl)-	0.00	0.09
	Phenol, 2,6-dimethoxy-4-(2-propenyl)-	0.00	0.08
	(E)-2,6-Dimethoxy-4-(prop-1-en-1-yl)phenol	0.96	0.22
Aromatics	Naphthalene	0	0.19
Alkanes	1,3-Cyclohexadiene, 1,5,5,6-tetramethyl-	0	0.1
Nitrogens	3,5-Dimethylpyrazole	0	0.59

Table S2 Elemental analysis of biochar and ACs of willow branch

Sample	**Ash (%)**	**Mass% organic basis**				**C/O ratio**	**C/H ratio**	**HHV (MJ/Kg)**
		C	**H**	**O**	**N**			
WB-Char-900	9.8	74.3	0.93	14.9	0.08	6.6	6.7	24.7
WB-CaO-AC-900	7.6	74.5	2.3	15.6	-	6.4	2.7	26.4

Table S3 Environmental impacts, energy consumption, and resource depletion for production of the ACs

Factors	WB-CaO
Acidification ($kg\ SO_2\ eq$)	5.66E+04
Carcinogenics (CTUh)	3.79E+01
Ecotoxicity (CTUe)	5.54E+08
Eutrophication (kg N eq)	4.32E+04
Fossil fuel depletion (MJ surplus)	9.95E+06
Global warming ($kg\ CO_2\ eq$)	1.37E+07
Non carcinogenics (CTUh)	1.37E+01
Ozone depletion (kg CFC-11 eq)	8.28E-01
Respiratory effects (kg PM2.5 eq)	1.98E+04
Smog ($kg\ O_3\ eq$)	8.05E+05

Table S4 Input and output on the basis of processing 1 ton of willow branch

WB-CaO		
Input/Output	**Quantity**	**Unit**
Step 1: Transportation		
Input		
Feedstock	1000	kg
transportation	1	tkm
Output		
Feedstock after transportation	990	kg
Step 2: Pretreatment		
Input		
Feedstock after transportation	990	kg
Water	2970	kg
Electricity	1425.6	MJ
Output		
Feedstock after pretreatment	940.5	kg
Waste water	2970	kg
Step 3: Grinding		
Input		
Feedstock after pretreatment	940.5	kg
CaO	940.5	kg
Electricity	149	MJ
Output		

Feedstock after grinding	1787.0	kg
Step 4: Pyrolysis		
Input		
Feedstock after grinding	1787.0	kg
Natural gas	410.9	m^3
Electricity	6.4	MJ
Output		
Biochar	1045.4	kg
Bio-oil	387.8	kg
H_2	26.3	kg
CO	192.1	kg
CO_2	57.9	kg
CH_4	67.0	kg
C_2H_4	10.5	kg
Step 5: Activation		
Input		
Biochar	1045.4	kg
Electricity	9.4	MJ
Natural gas	699.3	m^3
Output		
Solid	775.7	kg
Bio-oil	5.2	kg
H_2	4.3	kg
CO	167.3	kg

CO_2	92.0	kg
CH_4	0.9	kg
Step 6: Post-treatment		
Input		
Solid	775.7	kg
HCl	267.4	kg
Water	2327.0	kg
Electricity	131.8	MJ
Output		
AC	565.5	kg
Waste water	2327.0	kg

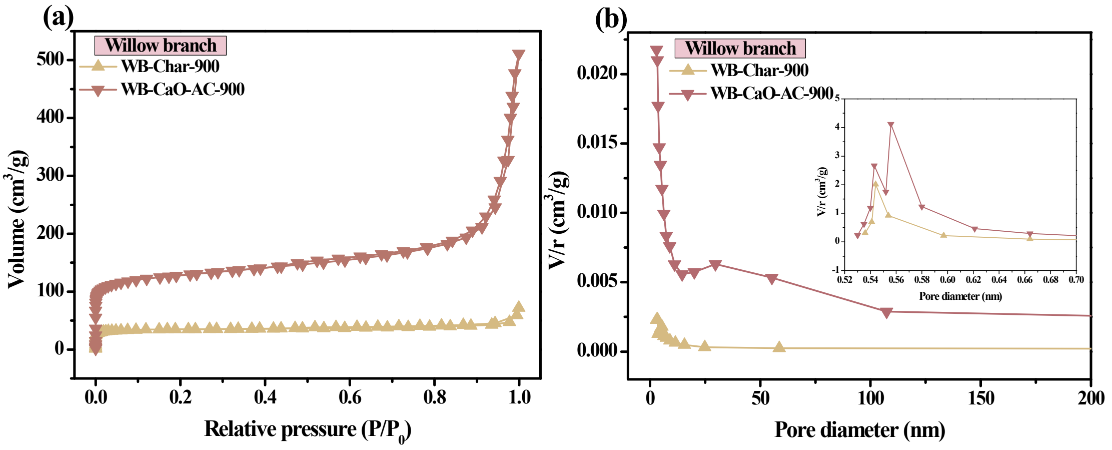

Figure S1 N_2 adsorption/desorption isothermal curves (a) and volume distribution diagram of BJH (b) of biochars and ACs from the subsequent activation of willow branch with/without CaO at 900°C

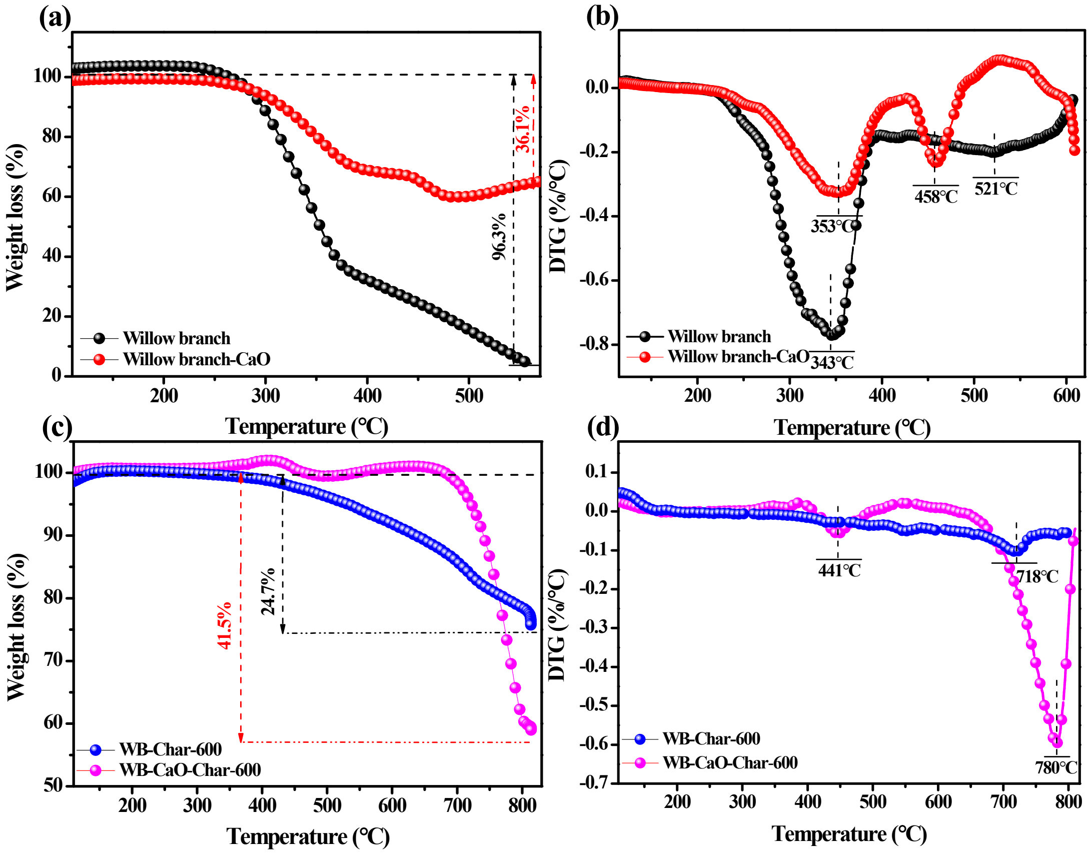

Figure S2 Thermal stability of the biochars and ACs. (a-b) TG and DTG curves of willow branch with/without CaO; (c-d) TG and DTG curves of willow branch derived biochar with/without CaO.

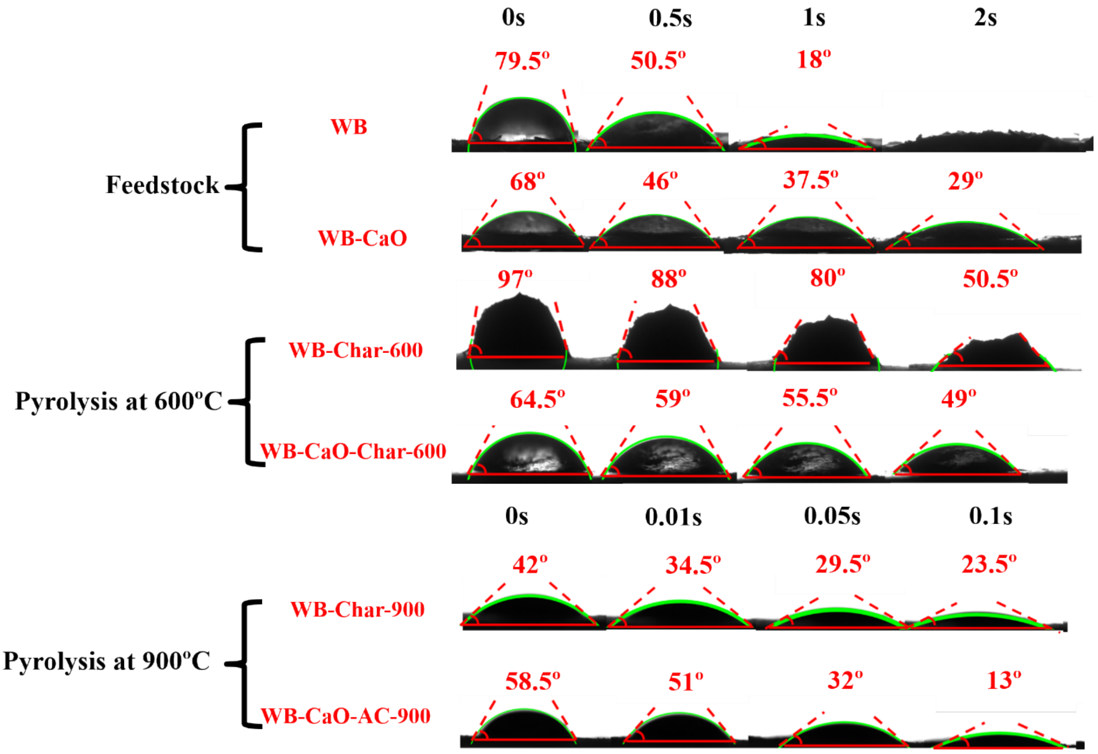

Figure S3 Contact angle characterization of willow branch feedstock and biochar from the pyrolysis of willow branch with/without CaO at 600° C and biochars and ACs from the subsequent activation of willow branch derived char with/without CaO at 900°C.

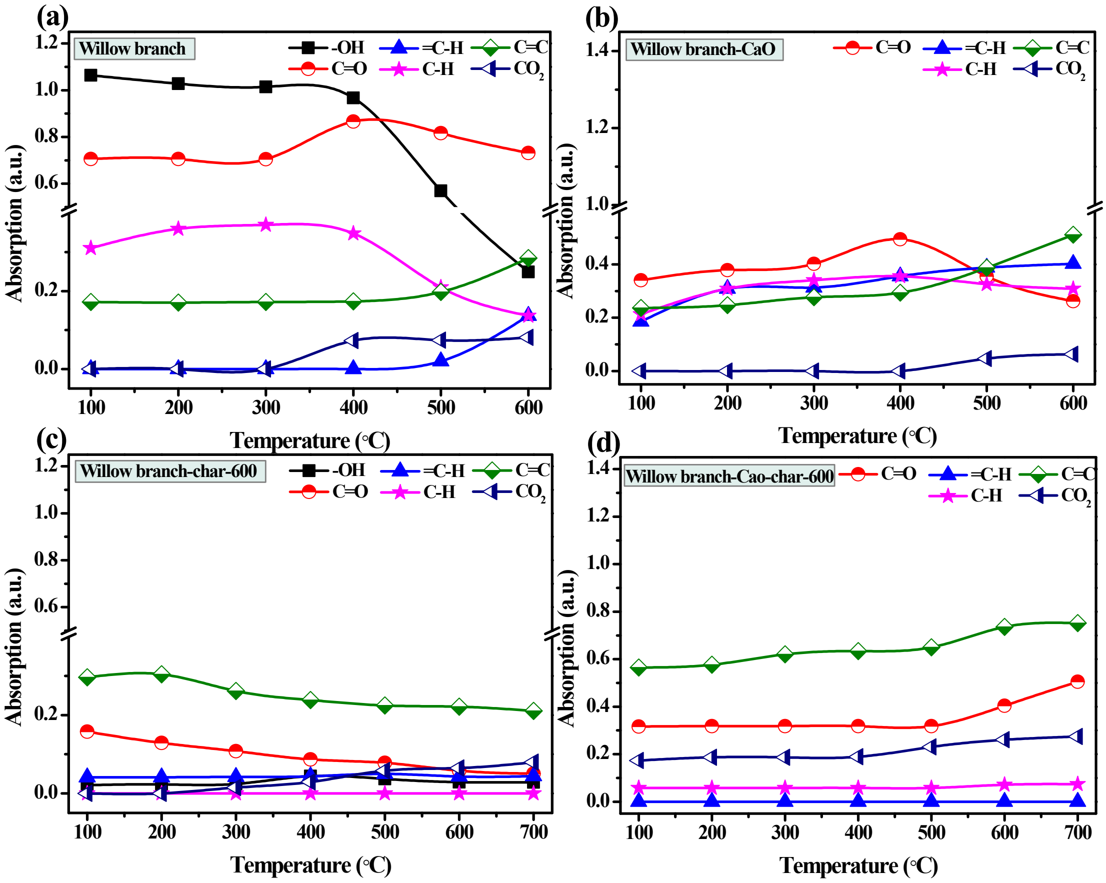

Figure S4 Evolution of various functionalities versus increasing temperature in in-situ DRIFTS spectra. (a): Pyrolysis of willow branch; (b): Pyrolysis of the mixture of willow branch and CaO; (c) Subsequent activation of willow branch derived char; (d) Subsequent activation of mixture derived char.